Separation Science and Technology
Publication details, including instructions for authors and subscription information:
http://www.informaworld.com/smpp/title~content=t713708471

Influence of Fluid Distribution on the Ultrafiltration Performance of a Ceramic Flat Sheet Membrane

C. Gaucher[a]; P. Jaouen[a]; P. Legentilhomme[a]; J. Comiti[a]
[a] GEPEA, Laboratoire de Génie des Procédés-Environnement-Agroalimentaire, Saint-Nazaire cedex, France

Online publication date: 15 April 2003

To cite this Article Gaucher, C. , Jaouen, P. , Legentilhomme, P. and Comiti, J.(2003) 'Influence of Fluid Distribution on the Ultrafiltration Performance of a Ceramic Flat Sheet Membrane', Separation Science and Technology, 38: 9, 1949 — 1962
To link to this Article: DOI: 10.1081/SS-120020128
URL: http://dx.doi.org/10.1081/SS-120020128

MARCEL DEKKER, INC. • 270 MADISON AVENUE • NEW YORK, NY 10016

SEPARATION SCIENCE AND TECHNOLOGY
Vol. 38, No. 9, pp. 1949–1962, 2003

Influence of Fluid Distribution on the Ultrafiltration Performance of a Ceramic Flat Sheet Membrane

C. Gaucher, P. Jaouen, P. Legentilhomme,* and J. Comiti

GEPEA, Laboratoire de Génie des Procédés-Environnement-Agroalimentaire, UMR-CNRS 6144, CRTT, Saint-Nazaire cedex, France

ABSTRACT

The limiting permeation flux and the cake resistance are determined during ultrafiltration experiments of a low concentrated suspension of glass microparticles at a plane ceramic membrane surface for three inlet and outlet configurations with different forms and cross sections. The limiting permeation flux values are analyzed in view of wall shear rates local values obtained in previous work.[1] The ratio of the inlet velocity to the mean tangential one appears to be a key parameter for understanding the performance of the ultrafiltration process. Indeed, a ratio value different from 1 leads to an increace of the limiting permeation flux and a decrease of the specific energy consumption. Furthermore, it seems that the limiting permeation flux value depends not only on the wall shear stress values, but also on the granulometric distribution of the deposit.

*Correspondence: P. Legentilhomme, GEPEA, Laboratoire de Génie des Procédés-Environnement-Agroalimentaire, UMR-CNRS 6144, CRTT, Boulevard de I'Universite, BP 406, Saint-Nazaire cedex 46602, France; E-mail: legenti@gepea.univ-nantes.fr.

DOI: 10.1081/SS-120020128 0149-6395 (Print); 1520-5754 (Online)

Key Words: Ultrafiltration; Plane ceramic membrane; Wall shear stress; Fluid distribution; Fouling.

INTRODUCTION

Crossflow ultrafiltration is a widely used technique for phase separation of many types of complex mixtures containing simultaneously solutes and particles. A major obstacle to these applications is the decline of the permeation flux due to concentration polarization and fouling during the filtration process. Characteristics of this deposit depend on the suspension composition, the membrane properties, and the operating conditions. Its formation and evolution have a direct effect on the filtration flux decline.

Bouzerar et al.[2] studied several inlet and outlet configurations of a filtration module consisting of a rotating disk inside a cylindrical housing fitted with a fixed-plate membrane. They showed that the permeation flux depends on the entrance and exit configurations. Therefore, among the different systems tested, the best configuration was that involving an inlet on the back plate and an axial outlet. The inlet and outlet configuration appears to be an important parameter to increase wall shear stress at the membrane surface without increasing the fluid velocity.

In a previous work,[3] the influence of the channel height and of the inlet and outlet configurations was studied using an electrochemical method. The investigation of the influence of the design of the distributors on the wall shear stress was obtained.[4]

The aim of the present work was to investigate the influence of fluid distribution on the ultrafiltration performance at a plane ceramic membrane. The interest of the plane ceramic membrane is to offer to the end user both the advantages of ceramic material and flat geometry. The main advantages are the equipment costs and good resistance at extreme pH and high temperatures. In this work, three distributors of different forms and different inlet and outlet sections are studied, following the conclusion of previous work involving other inlet and outlet configurations.[1]

MATERIALS AND METHOD

The same experimental set-up as that described in our previous work[1] is used in the present study. The electrolytic solution was thermostated at 30°C in the feed tank to keep its physical properties constant during all

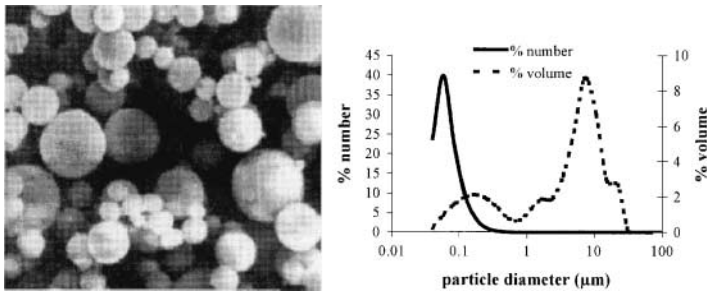

Figure 1. Granulometric distribution of the initial suspension.

the experiments. The fluid was brought to the circuit by a centrifugal-type pump to ensure a constant tangential velocity at the plane surface. The flow rates were measured using a rank of two flowmeters. The filtration can be conducted under constant differential pressure conditions of 50 kPa, using a second pump and a pressure throttling valve installed at the outlet side of the membrane module. The permeate and the retentate were returned to the feed tank to keep a constant concentration of particles during the ultrafiltration process. Two concentrations were investigated: 1 and 5 $g.L^{-1}$.

The ceramic plane ultrafiltration membrane is sold commercially by Tami Industries (Nyons, France) with a 150 kDa molecular weight cut-off and a total surface area of 0.015 m^2. The suspension was made of glass microparticles, the granulometric distribution of which is presented in Fig. 1. It was obtained

Table 1. Description of the different distributors investigated.

Distributor shape	Description	U_{inlet}/U_{module}
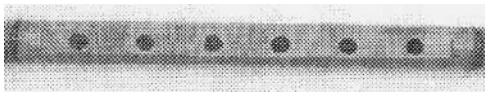	Six holes of same diameter $d = 6$ mm	0.72
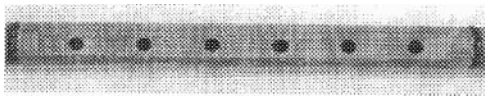	$d = 5$ mm	1.03
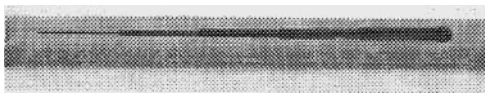	Distributor of trapezoidal shape	2.13

using a laser granulometer (Coulter LS 230, Coultronics-Beckmann, Margency, France). The density of the glass particles was $1100 \pm 50\,kg.m^{-3}$.

The three designs of distributors were described in previous work.[1] Those three distributors were chosen according to the criterion that they present a ratio of the inlet velocity to the mean tangential one, greater, lower, or nearly equal to one, inducing a decrease, an increase, or no change of the mean tangential velocity in the module compared with that in the inlet itself (Table 1).

RESULTS AND DISCUSSION

Effect of the Distributor Shape

Figure 2 represents the permeation flux versus time for three values of the Reynolds number. At a low Reynolds number value (Re = 179), the permeation flux is stabilized faster (after about 30 minutes of processing). At a higher Reynolds number (Re = 1380), the permeation flux slowly decreases until a stable value is reached after about 180 minutes. Thus, all the experimental values of the permeation flux are taken after 180 minutes of filtration and represent the limiting permeation flux, J_{lim}.

Figure 3 represents the dimensionless limiting permeation flux, J_{lim}/J_0, where J_0 is the pure water permeation flux, and the average wall shear rates, $\bar{S}$, measured without particles,[1] vs. the Reynolds number for the same particle concentration of $1\,g.L^{-1}$ and a transmembrane pressure of 50 kPa. The wall shear rate values were determined at the surface of the plane ceramic

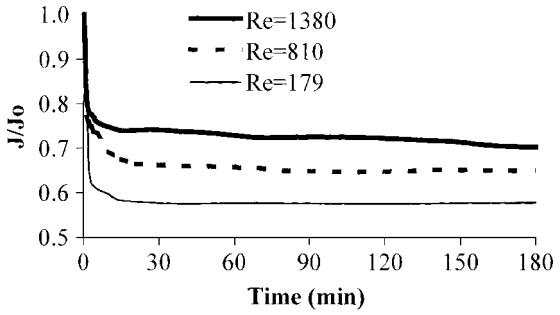

Figure 2. Permeation flux vs. time for three Reynolds numbers and the distributor of trapezoidal shape. $P_{TM} = 50\,kPa$, $T = 30°C$, and $C = 1\,g.L^{-1}$.

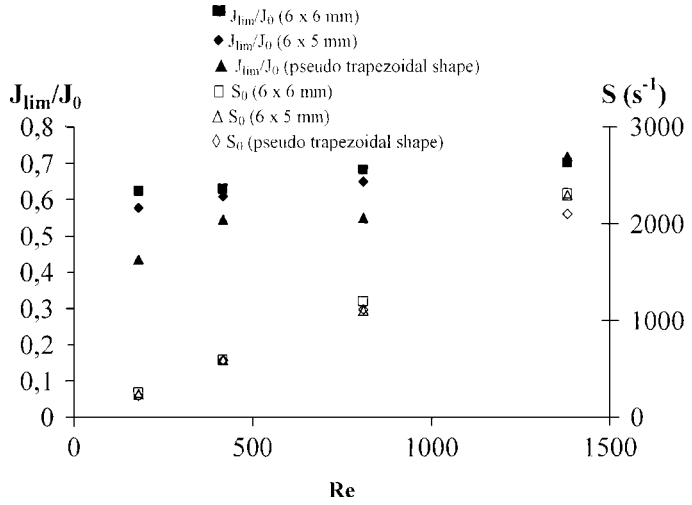

Figure 3. Dimensionless limiting permeation flux and wall shear rate vs. Reynolds number for the three distributors.

ultrafiltration membrane using an electrochemical method described in previous work.[1]

Results obtained regarding limiting flux and average wall shear rate are nearly equal, whatever the shape of the distributor. At a Reynolds number less than 1000, J_{lim}/J_0 values are slightly greater for the distributor consisting of six holes, 6 mm in diameter than for the distributor of pseudo trapezoidal shape. The lowest values are obtained for the six holes of 5 min diameter distributor, for which the ratio $U_{inlet}/U_{module} = S_{module}/S_{inlet}$ (see Table 1) is nearly equal to one. At a Reynolds number equal to 1380, the performance of the three distributors are nearly identical. It seems that a change of the mean tangential velocity in the module as compared to the inlet velocity (increase or decrease of the mean tangential velocity) induces greater permeation flux and, consequently, enhances the filtration efficiency. If limiting flux and average velocity gradients are compared at a Reynolds number less than 1380, we observe that the distributor of pseudotrapezoidal shape and that consisting of six holes of 6 mm allow the obtainment of a slightly greater limiting permeation flux than the distributor consisting of six holes of 5 mm in diameter. The average velocity gradient is similar. Thus, in this case it seems that the wall shear rate does not influence the limiting permeation flux values because the difference between wall shear rate values

obtained for the three inlet and outlet configurations is really weak; whereas, a change in the limiting permeation flux is observed.

Effect of Feed Concentration

Figure 4 represents the dimensionless limiting flux obtained for the distributor of trapezoidal shape and two particle concentrations and the average velocity gradients obtained without particles[1] vs. the Reynolds number. Logically, limiting permeation flux decreases when the concentration is increased. Furthermore, for a concentration of $5\,g.L^{-1}$, the increase of Re does not induce a great difference in the level of the limiting flux. This can be explained by the structure of the deposit. Figure 5 represents the granulometric distribution of the deposit for the two concentrations and two Reynolds numbers (179 and 1380). According to this figure, we observe that the more the concentration of particles is increased, the more the deposit is constituted of small particles (circled zone). This structure of the deposit induces a greater flow resistance and thus, can be the cause of the strong decrease of flux despite a small difference in velocity gradient. Furthermore, increase of the Reynolds number induces an increase of the number of small particles in the deposit for a same concentration (circled zone). This phenomenon can explain the small differences between limiting flux for a concentration of $5\,g.L^{-1}$ when the Reynolds number is increased. Indeed, despite the change of flow characteristics when the Reynolds number increases, the deposit constituted of small particles induces a more important flow resistance and decreases the permeation limiting flux. Our results are in agreement with those of Chellam and Wiesner,[5] who have shown that the small particle are less sensible to the wall shear stress effects. The large particles are more easily dragged toward the bulk suspension (principle of the free turbulence promoters).

Cake Resistances

Darcy's law allows the determination of the cake resistance due to the particles deposit:

$$J_{\text{lim}} = \frac{P_{TM}}{\mu(R_m + R_c)} \tag{1}$$

where P_{TM}, R_m, and R_c represent the transmembrane pressure, the intrinsic membrane resistance, and the cake resistance, respectively.

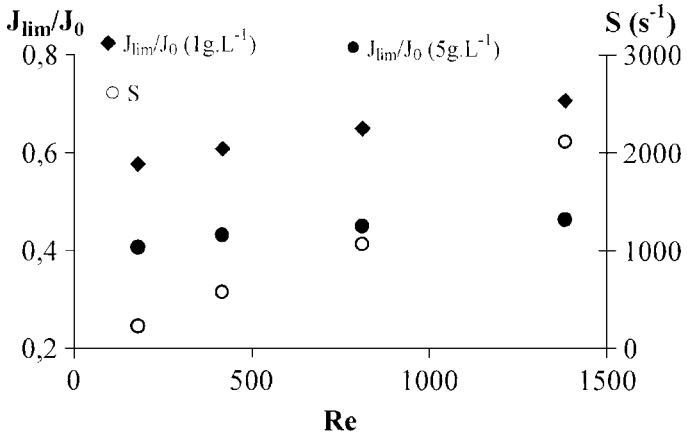

Figure 4. Dimensionless limiting permeation flux and wall shear rate vs. Reynolds number for the distributor of trapezoidal shape and two concentrations.

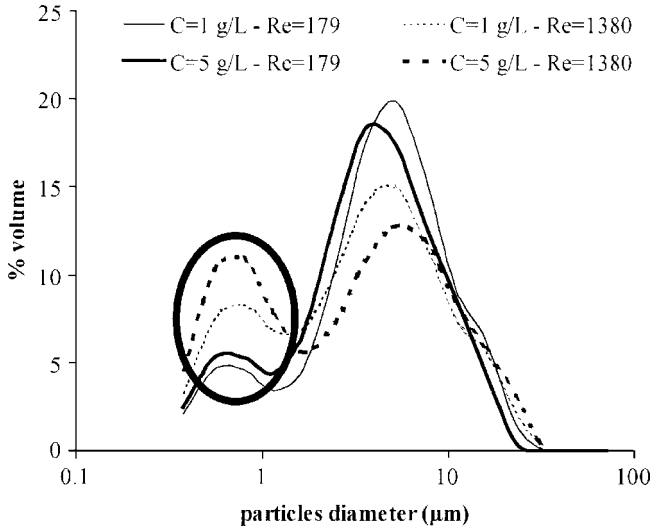

Figure 5. Granulometric distribution in volume of the cake deposit obtained at the end of the ultrafiltration process with the distributor of trapezoidal shape and two concentrations.

The pure water flux, J_0, can be expressed by:

$$J_0 = \frac{P_{TM}}{\mu \cdot R_m} \tag{2}$$

thus,

$$R_c = R_m \left(\frac{J_0}{J_{\text{lim}}} - 1 \right) \tag{3}$$

The membrane resistance was calculated during filtration without particles, $R_m = 2.8\ 10^{12}\,\text{m}^{-1}$. Then, for each experiment, the cake resistance was determined (Fig. 6). The cake resistance values are in agreement with the limiting permeation fluxes. Indeed, the lower the cake resistance, the higher the limiting permeation flux, the deposit induces a lower resistance to flow. The distributor consisting of six holes of 5 mm in diameter causes higher cake resistance than the other ones for a Reynolds number less or equal to 810. Then, when the Reynolds number is about 1380, this difference decreases. Thus, the hydrodynamic changes seem to dump the influence of inlet and outlet configurations.

To quantify the real effect of the deposit, the specific cake resistance, r_c, is calculated:

$$r_c = \frac{R_c}{\delta} \tag{4}$$

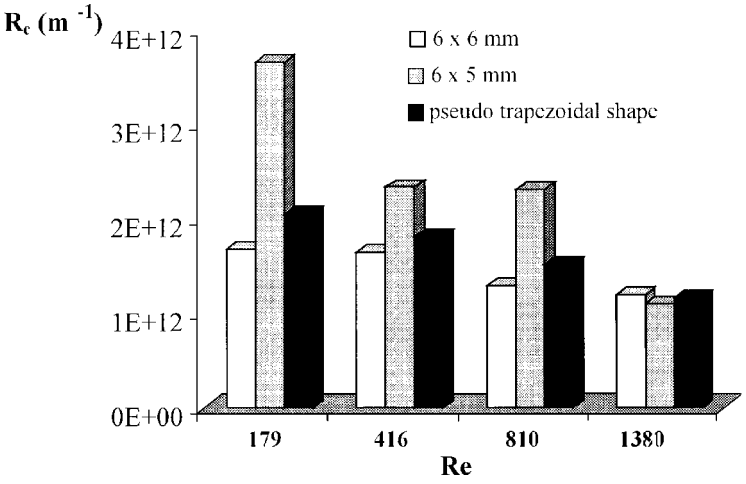

Figure 6. Cake resistance vs. Reynolds number for the three distributors. $P_{TM} = 50\,\text{kPa}$, $T = 30°\text{C}$, and $C = 1\,\text{g.L}^{-1}$.

where δ represents the deposit thickness, determined by using an electrochemical method based on the measurement of the limiting electrodiffusional current on microprobes inserted at the surface of the ceramic membrane. This experimental technique was detailed in previous work.[6]

The specific resistance of a filter cake is often considered as a measurement of the difficulty for a fluid to pass through a filter. This case can be related to the deposit characteristics using the Koseny–Carman equation in the Darcy flow regime. This equation describes the fluid permeation through particle layers or porous media in the laminar regime:

$$J_o - J_{lim} = \frac{d_p^2.\varepsilon^3}{180\mu(1-\varepsilon)^2}\frac{P_{TM}}{\delta} \tag{5}$$

From Eqs. (1) and (5), the specific cake resistance becomes:

$$r_c = \frac{R_c}{\delta} = \frac{180(1-\varepsilon)^2}{d_p^2.\varepsilon^3} \tag{6}$$

Thus, the specific cake resistance depends only on the deposit characteristics (porosity, ε, and surface equivalent particle diameter, d_p) and not on the deposit thickness.

The mean porosity of the cake layer was estimated for the distributor of pseudotrapezoidal shape in previous work[6] using an electrochemical method.

Figure 7 represents the specific cake resistances for different configurations, Reynolds numbers, and concentrations. The specific cake resistance increases when the Reynolds number is increased, with the exception of the distributor with six holes of 5 mm in diameter, which increased at a Reynolds number equal to 1380. Our results are in agreement with the conclusions of Chellam and Wiesner,[5] who have found that for a given feed suspension cake, specific resistances increase with the entrance shear rate, suggesting that cakes formed at higher entrance shear rates are more compact. For the distributor of pseudotrapezoidal shape, the porosity obtained at Reynolds numbers equal to 179 and 1380 did not change and is equal to 0.41. Thus, the increase of the specific resistance with the Reynolds number is due to the decrease of the mean diameter of the deposited particles. So, the granulometric distributions of the deposits have been investigated. To study the granulometric patterns of the particles deposits, those collected were analyzed using a laser granulometer. The granulometric distribution, presented in Fig. 5, confirms this result, showing more small particles in the deposit at a higher Reynolds number.

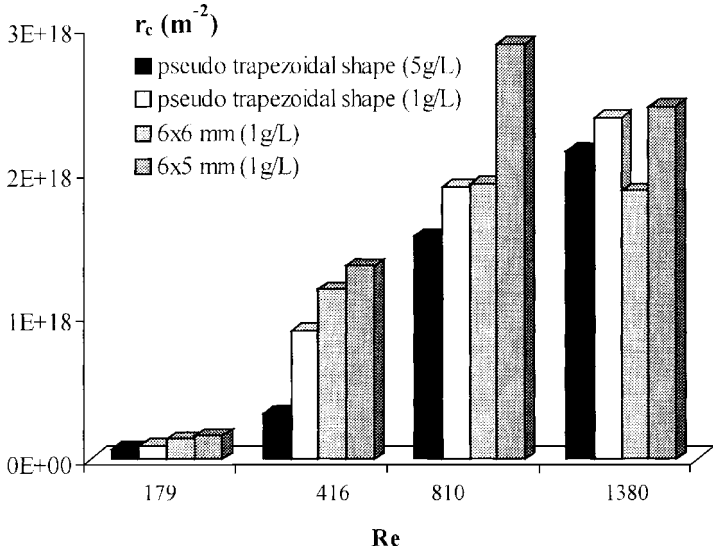

Figure 7. Specific cake resistance vs. Reynolds number for the three distributors.

Four assumptions are required to ensure the validity of the Koseny–Carman equation: (i) uniform particle size, (ii) laminar flow through the pores, (iii) validity of Darcy's law, and (iv) absence of long-and short-range forces of interaction. The second and third assumptions are reasonable for the flow through the cake layer during filtration. The fourth assumption is satisfied because the particles used are made of glass. The first assumption is the most questionable one, because of the polydispersion of the suspension size, thus the mean diameter, d_p, that we can obtained from the granulometric distribution of the deposit, is not necessarily the one that has to be used in Kozeny–Carman equation valid for monodispersed particles.

MacDonald and Chu[7] derived a generalized Koseny–Carman equation to estimate the permeability of particle beds consisting of polydispersed spheres. Following this work, the specific resistance can be expressed by the following equation for a polydispersed suspension:

$$r_c = \frac{9\pi^2}{2} \cdot \frac{(1-\varepsilon)^2}{\varepsilon^3 \cdot d_p^2} \tag{7}$$

Lee and Clark[8] have shown that the theoretical prediction of the Koseny–Carman equation tends to underestimate the specific cake resistance

for large particle sizes, whereas, it leads to an overestimation for smaller particle sizes.

Indeed, the porosity values and the particle diameters change when hydrodynamics is modified. Furthermore, the increase of the concentration induces a decrease of the specific cake resistance (increase of porosity or/and surface equivalent particle diameter). This phenomenon can explain the small differences of limiting permeation flux between the experiments realized at $1\,g.L^{-1}$ and those made at a concentration of $5\,g.L^{-1}$. Indeed, the limiting permeation flux depends on the deposit thickness and also on the deposit characteristics.

Energy Requirements

The total energy, W, required for ultrafiltration is the sum of several contributions[9]:

$$W = W_T + W_F + W_R \tag{8}$$

were W_T is the thermal energy required to maintain the processing fluid temperature. The temperature of the suspension in the experiment was maintained constantly using a thermoregulator. The thermal energy was not taken into account in our energy estimations. W_F is the energy required by the feed pump for maintaining the transmembrane pressure, measured by means of two manometers placed at the inlet and at the outlet of the module, respectively, W_R is the energy needed by the recirculating pump to maintain the fluid velocity throughout the module. In ultrafiltration applications, W_F is often considered as low compared to W_R.[9]

W_F and W_R were expressed vs. the permeate volume during the entire ultrafiltration time (m^3 of permeate) in terms of $k.W.h$ per m^3 of permeate:

$$W_F = \frac{Q_F \cdot P_o}{\eta_F J_{\lim} \cdot A_m} \tag{9}$$

where Q_F, η_F, and A_m represent the feed flow rate, the efficiency of the feed pump, and the membrane surface, respectively.

$$W_R = \frac{Q \cdot \Delta P}{\eta_R \cdot J_{\lim} \cdot A_m} \tag{10}$$

Where Q, η_R, and ΔP represent the tangential flow rate, the efficiency of the recirculating pump, and the pressure drop between the inlet and the outlet of the module ($\Delta P = P_i - P_o$). The pressure drop between the inlet and

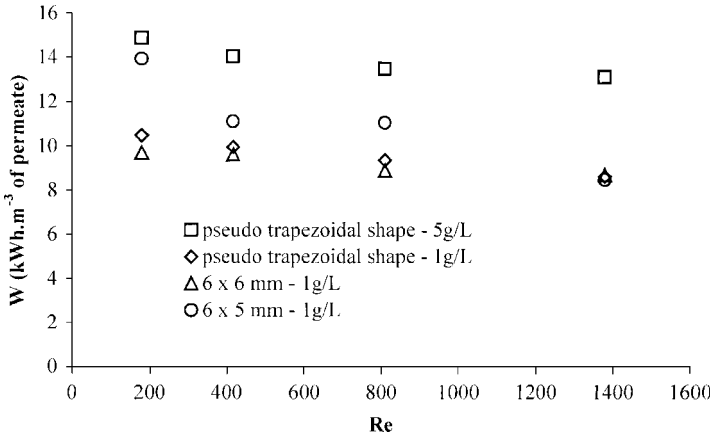

Figure 8. Total energy per m^3 of permeate vs. Reynolds number for the three distributors.

the outler of the module is weak for the three shapes of distributors for a same Reynolds number and concentration. The maximum value obtained is about 5 kPa for the highest Reynolds number investigated.

Figure 8 represents the total energy, *W*, for the different inlet and outlet configurations. This figure shows a difference of about 20% between the energy required by the distributor with six holes of 5 mm in diameter and the configurations with six holes of 6 mm and that of trapezoidal shape for the ultrafiltration of a suspension concentrated at $1\,g.L^{-1}$ at low Reynolds numbers. Thus the differences in the total energy is only linked on the flux for the same Reynolds numbers and concentrations. It seems that a change of the tangential velocity compared to the inlet velocity (acceleration or deceleration) decreases the energy consumption for low tangential velocities.

CONCLUSION

The ratio of the inlet velocity to the mean tangential velocity seems to be an important parameter to optimize ultrafiltration performance. Indeed, when it is different from 1, inducing an increase or a decrease of the mean tangential velocity compared with that in the inlet, the limiting permeation flux value increases and the specific energy consumption decreases. Thus, it seems interesting to keep a ratio of velocities away from unity. This parameter has to

be considered for the conception of a plane module, because for the ultrafiltration of viscous or charged suspensions, the channel heights is generally increased. This increase leads to a decrease of the mean tangential velocity and, consequently, to a change of the the ratio of the characteristic velocities. It seems interesting to change the inlet velocity, changing the inlet section, to keep a ratio of characteristic velocities rather different from unity.

NOMENCLATURE

A_m	membrane surface, m^2
d_p	surface equivalent particle diameter, m
e	module thickness, m
J_{lim}	limiting permeation flux, $m.s^{-1}$
J_0	water permeation flux, $m.s^{-1}$
L	module length, m
P_i	inlet module pressure, Pa
P_o	outlet module pressure, Pa
P_{TM}	transmembrane pressure, Pa
ΔP	pressure drop along the module, Pa
Q	tangential flow rate, $m^3.s^{-1}$
Q_F	feed flow rate, $m^3.s^{-1}$
r_c	specific cake resistance, m^{-2}
R_c	cake resistance, m^{-1}
R_m	membrane resistance, m^{-1}
$\bar{S}$	average wall shear rate, s^{-1}
S_{inlet}	inlet section, m^2
S_{module}	module section, m^2 ($S_{module} = L.e$)
U_{inlet}	inlet velocity, $m.s^{-1}$
U_{module}	mean tangential velocity in the module, $m.s^{-1}$
W	total energy, $kW.h.m^{-3}$
W_F	energy required by the feed pump, $kW.h.m^{-3}$
W_R	energy required by the recirculating pump, $kW.h.m^{-3}$
W_T	thermal energy, $kWh.m^{-3}$

Greek Letters

δ	cake thickness, m
ε	cake porosity
μ	dynamic viscosity, Pa.s
η_F	yield of the feed pump
η_R	yield of the recirculating pump

REFERENCES

1. Gaucher, C.; Jaouen, P.; Legentilhomme, P.; Comiti, J. Suction effect on the shear stress at a plane ultrafiltration ceramic membrane surface. Sep. Sci. Technol. **2002**, *37* (10), 2251–2270.
2. Bouzerar, R.; Jaffrin, M.Y.; Ding, L.; Paullier, P. Influence of geometry and angular velocity on performance of a rotating disk filter. AIChE J. **2000**, *46* (2), 257–265.
3. Gaucher, C.; Legentilhomme, P.; Jaouen, P.; Comiti, J.; Pruvost, J. Hydrodynamics study in a plane ultrafiltration module using an electrochemical method and particle image velocimetry vizualisation. Exp. Fluids **2000**, *32*, 283–293.
4. Gaucher, C.; Legentilhomme, P.; Jaouen, P.; Comiti, J. Influence of the fluid distribution on the wall shear stress in a plane ultrafiltration module using an electrochemical method. Trans. IchemE. Chem. Eng. Res. Des. **2002**, *80*, 111–120.
5. Chellam, S.; Wiesner, M.R. Evaluation of cross-flow filtration models based on shear-induced diffusion and particle adhesion: complications induced by feed suspension polydispersivity. J. Memb. Sci. **1998**, *138*, 83–97.
6. Gaucher, C.; Jaouen, P.; Comiti, J.; Legentilhomme, P. Determination of cake thickness and porosity during cross-flow ultrafiltration on a plane ceramic membrane surface using an electrochemical method. J. Memb. Sci. **2002**, *210*, 245–258.
7. MacDonald, M.J.; Chu, C.-F.; Guilloit, P.P.; Ng, K.M. A generalized Blake-Kozeny equation for multisized spherical particles. AIChE J. **1991**, *37*, 1583–1588.
8. Lee, Y.; Clark, M.M. Modeling of flux decline during cross-flow ultrafiltration of colloidal suspensions. J. Memb. Sci. **1998**, *149*, 181–202.
9. Sharma, D.K.; Reuter, H. Quarg-making by ultrafiltration using polymeric and mineral membrane modules: a comparative performance study. Lait **1993**, *73*, 303–310.

Received August 2002
Revised December 2002